A Novel Robust Attitude Control for Quadrotor Aircraft Subject to Actuator Faults and Wind Gusts

Yuying Guo, Bin Jiang, *Senior Member, IEEE,* and Youmin Zhang, *Senior Member, IEEE*

***Abstract*—A novel robust fault tolerant controller is developed for the problem of attitude control of a quadrotor aircraft in the presence of actuator faults and wind gusts in this paper. Firstly, a dynamical system of the quadrotor taking into account aerodynamical effects induced by lateral wind and actuator faults is considered using the Newton-Euler approach. Then, based on active disturbance rejection control (ADRC), the fault tolerant controller is proposed to recover faulty system and reject perturbations. The developed controller takes wind gusts, actuator faults and measurement noises as total perturbations which are estimated by improved extended state observer (ESO) and compensated by nonlinear feedback control law. So, the developed robust fault tolerant controller can successfully accomplish the tracking of the desired output values. Finally, some simulation studies are given to illustrate the effectiveness of fault recovery of the proposed scheme and also its ability to attenuate external disturbances that are introduced from environmental causes such as wind gusts and measurement noises.**

***Index Terms*—Active disturbance rejection control (ADRC), attitude control, actuator faults, disturbances rejection, quadrotor aircraft.**

I. Introduction

RECENT scientific innovations and improvements have boosted the utilization of unmanned aerial vehicles (UAVs) in a large and expanding number of applications such as law enforcement [1], marine operations [2], battle damage assessment [3], agriculture services [4], mapping and photographing [5], wild fire surveillance [6], [7], inspection of buildings and bridges [8], surveillance over nuclear reactors [9] and power lines [10]. Due to the requirements of autonomous flight under different flight conditions without a pilot onboard, control of UAV flight is much more challenging compared with manned aerial vehicles since all operations have to be carried out by the automated guidance, navigation and control (GNC) algorithms embedded on the onboard flight microcomputer/microcontroller or with limited interference by a ground pilot if needed. Moreover, during all these missions, the precise attitude control combined with wind gusts attenuation capabilities and the enhanced reliability and safety of complex and autonomous systems due to occurrence of faults are necessarily required. So, an effective yet easy to implement controller, which has the capability of ensuring its effectiveness even in the presence of actuator faults and strong disturbances, is required.

For the quadrotor helicopter, as an example of UAV systems, which is relatively a simple, affordable and easy to fly system, the accurate attitude control of it in harsh environmental conditions due to wind disturbances is an open challenge. Particularly, robustness issues can be critical for the rotorcrafts due to the complicated aerodynamic effects (which make it difficult to obtain an accurate dynamic model), such as the errors from sensors (like measurement noises) and external disturbances (like winds). Many researches have addressed the design of proper attitude control strategies for quadrotor. Nevertheless, only a few studies about robust control of aircraft in the presence of wind can be found in the literature. In [11], a backstepping-based controller with input saturations for the hovering flight of a UAV was introduced and it was applied (in simulation) to an airship UAV in face of wind disturbances. The problem of UAV path planning with wind disturbances is discussed in [12], [13]. In [14], a novel nonlinear feedback control law is developed to compensate for modeling errors which can perform robustly against external perturbations such as wind gusts. Reference [15] and [16] account for wind gust disturbances, but only as linear perturbations. The quadrotor is a 6 degree-of-freedom (DOF) device with only four actuators, which makes it an under-actuated vehicle with unstable dynamics and highly coupled states. Moreover, due to load limitations, there is no hardware redundancy, so the enhanced reliability and safety of a quadrotor in the presence of faults is critical. Then, the development of an autonomous fault diagnosis [17] and recovery system [18]−[21] that can cope with these faults is necessarily needed. In [22], an adaptive PID controller is proposed for fault tolerant control of a quadrotor helicopter system in the presence of actuator faults, and a fuzzy logic controller is used to tune PID gains online where the tracking error and the change of the tracking error are used to determine control parameters. However, PID controllers are reliable with certain level of robustness to model uncertainties

Manuscript received August 22, 2016; accepted March 30, 2017. This work was supported by the National Natural Science Foundation of China (61573282), the Foundation of the Education Department of Sichuan Province (16ZA0132), and the Foundation of Robot Technology Used for Special Environment, Key Laboratory of Sichuan Province (13zxtk06). Recommended by Associate Editor Yingmin Jia. *(Corresponding author: Yuying Guo.)*

Citation: Y. Y. Guo, B. Jiang, and Y. M. Zhang, "A novel robust attitude control for quadrotor aircraft subject to actuator faults and wind gusts," *IEEE/CAA J. of Autom. Sinica*, vol. 5, no. 1, pp. 292−300, Jan. 2018.

Y. Y. Guo is with the School of Information Engineering, Southwest University of Science and Technology, Mianyang 621010, China (e-mail: polarisguo@163.com).

B. Jiang is with the College of Automation Engineering, Nanjing University of Aeronautics and Astronautics, Nanjing 210016, China (e-mail: binjiang@nuaa.edu.cn).

Y. M. Zhang is with the Department of Mechanical, Industrial and Aerospace Engineering and the Concordia Institute of Aerospace Design and Innovation, Faculty of Engineering and Computer Science, Concordia University, Montreal, Quebec H3G 1M8, Canada (e-mail: ymzhang@encs.concordia.ca).

Color versions of one or more of the figures in this paper are available online at http://ieeexplore.ieee.org.

Digital Object Identifier 10.1109/JAS.2017.7510679

and disturbances. Moreover, when the control input is a step signal, the output of system cannot be step due to the inertia of the system, and there will be large initial error. Model predictive control (MPC) is a promising tool for fault tolerant control applications [23] due to its prominent capabilities such as constraint handling, flexibility to changes in the process dynamics and applicability to nonlinear dynamics. However, MPC needs an almost explicit model of the system to calculate a stabilizing control signal, meanwhile, the abrupt changes in the model parameters, due to failure, cannot be predicted beforehand and an online data-driven parameter estimation methodology is required. Sliding mode control (SMC) and backstepping techniques have also been used in [24] and [25], and in these works the convergence of the quadrotor internal states is guaranteed; however, the computations required are relatively excessive.

Given that the quadrotor is an under-actuated system, the possible set of available solutions for control and fault recovery is rather limited. Moreover, in real world applications there are always measurement noises and wind gusts. Also, to the best of authors' knowledge, there are no fault recovery methods based on active disturbance rejection control (ADRC) presented for a quadrotor aircraft in literature, therefore, the main objective of this paper is to develop fault tolerant control methods that are effective, simple to implement and robust to model uncertainties and external disturbances for quadrotor control system in the presence of actuator faults, wind gusts and measurement noises by ADRC initiated by Han [26]. In contrast to previous methods, the developed fault tolerant control method is a remarkable control strategy for four reasons: 1) it is a robust control strategy, where the model of quadrotor is extended with a new state variable, which includes all unknown dynamics and disturbances that are left unnoticed in the normal plant description and is online estimated using a state observer called extended state observer (ESO); 2) the online estimation of the new state is used to separate the system and the gentle disturbances, which in turn indirectly simplifies the model to a large extent, and the real time compensation of the uncertainty also reduces the trouble in its modelling; 3) discrepancies in modelling will not affect the control mechanism, as this technique involves inclusion of all uncertainties as the extended state variable; 4) robustness and uncertainty reduction ability of this method makes it an interesting solution in scenarios where the full knowledge of the system is not available.

The construction of this paper is organized as follows: In Section II, a nonlinear dynamic model with actuator faults and wind gusts is derived. The fault tolerant method based on ADRC is developed in Section III. To analyze the performance of the developed fault tolerant controller, several simulations are carried out and presented in Section IV. Conclusions and future work are finally discussed in Section V.

II. Quadrotor's Mathematical Model Subject to Actuator Faults and Wind Gusts

A. Preliminaries

A quadrotor aircraft is actuated by four rotors. The coordinate systems and free body diagram for the quadrotor are shown in Fig. 1. There are two reference frames subjected to the quadrotor: The earth-fixed frame $E = (O^E, x^E, y^E, z^E)$ and the body-fixed frame $B = (O^B, x^B, y^B, z^B)$. It is assumed that the body-fixed frame and the center of gravity of the quadrotor must coincide. A cross formed by two arms holds the four rotors, two rotors at the two ends of one arm rotate in the clockwise direction, while the other pair of rotors rotates in the opposite direction to cancel the yawing moment. To describe the behavior of the quadrotor, its absolute position vector is denoted as $\boldsymbol{\xi} = [x, y, z]^T \in E$ and attitudinal vector is denoted as Euler angles $\boldsymbol{\eta} = [\phi, \theta, \psi]^T \in E$. Euler angles are respectively roll angle ϕ, pitch angle θ, and yaw angle ψ with the assumption of $-\pi/2 < \phi < \pi/2$, $-\pi/2 < \theta < \pi/2$, $-\pi < \psi < \pi$. The linear motions along with x, y, z axes and rotating motion around the z-axis are accomplished by changing the speed of rotors properly. Control forces and moments are generated by varying the speed of the rotors $(\Omega_1, \Omega_2, \Omega_3, \Omega_4)$ as shown in Table I. In Table I, a $(+)$ symbol indicates that increasing the corresponding rotor speed generates a positive force/moment, while a $(-)$ symbol indicates that decreasing the corresponding rotor speed generates a positive force/moment. To get from E to B, we first rotate about z^E axis by the yaw angle, ψ, then rotate about the intermediate y^E axis by the pitch angle, θ, and finally rotate about the x^E axis by the roll angle, ϕ. The rotation matrix for transforming the coordinates from E to B is given by

$$R_\Omega = \begin{bmatrix} \cos\psi\cos\theta & -\sin\psi\cos\phi + \cos\psi\sin\theta\sin\phi & \sin\psi\sin\phi + \cos\psi\sin\theta\cos\phi \\ \sin\psi\cos\theta & \cos\psi\cos\phi + \sin\psi\sin\theta\sin\phi & -\cos\psi\sin\phi + \sin\psi\sin\theta\cos\phi \\ -\sin\theta & \cos\theta\sin\phi & \cos\theta\cos\phi \end{bmatrix}.$$

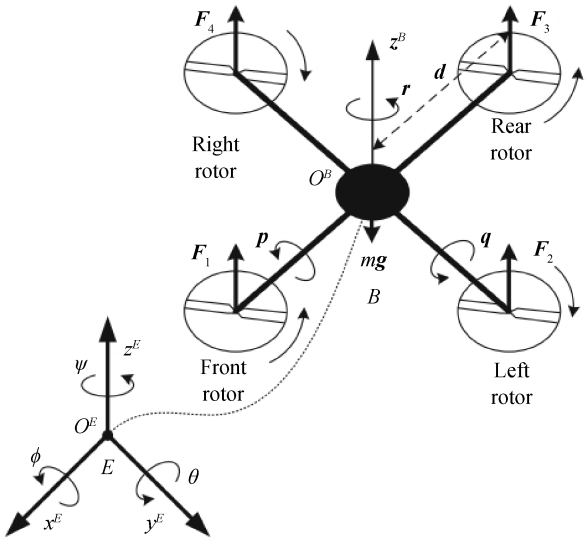

Fig. 1. Quadrotor model.

By using the Newton-Euler approach, the general mathematical model describing the dynamics of an aircraft evolving in a three-dimensional space is expressed in (1) [27],

TABLE I
VARIATION OF ROTOR SPEEDS TO GENERATE CONTROL FORCES AND MOMENTS

Force / Moment	Ω_1	Ω_2	Ω_3	Ω_4
Roll moment		–		+
Pitch moment	–		+	
Yaw moment	–	+	–	+
Vertical thrust	+	+	+	+

$$\begin{aligned}
&\dot{\boldsymbol{\xi}} = \boldsymbol{\nu}\\
&m\dot{\boldsymbol{\nu}} = \boldsymbol{F}\\
&\dot{R}_{\Omega} = R_{\Omega}\hat{\Omega}\\
&J\dot{\Omega} = -\Omega \times J\Omega + \Omega \times [0 \;\; 0 \;\; J_r\Omega_r] + \boldsymbol{\tau}
\end{aligned} \tag{1}$$

where $\boldsymbol{\nu}$ is the generalized velocity vector with respect to E-frame and Ω is the angular velocity expressed in B-frame, $\hat{\Omega}$ denotes the anti-symmetric matrix of Ω, m is the mass of the rigid body, J denotes the constant inertia matrix around the center of mass, $\boldsymbol{F} \in \boldsymbol{R}^3$ is non-conservative forces expressed in an inertia frame E, and $\boldsymbol{\tau} \in \boldsymbol{R}^3$ is torques applied to its center of mass and specified with respect to the body frame B. $\Omega \times [0 \;\; 0 \;\; J_r\Omega_r]$ denotes the gyroscopic effects produced by the propeller rotation, J_r is the total rotational moment of inertia around the propeller axis and Ω_r is the overall propellers' speed which is defined in (2),

$$\Omega_r = -\Omega_1 + \Omega_2 - \Omega_3 + \Omega_4. \tag{2}$$

B. Wind Gusts Modeling

In real world applications, a quadrotor is generally exposed to crosswind. A crosswind is defined as the wind which occurs perpendicular to the vehicle but parallel to the ground, i.e., the quadrotor is disturbed by lateral wind. If an aircraft is experiencing a crosswind, it will be pushed over or yawed away from the wind. Consequently, this leads to additional forces, f_{W_i}, acting over each rotor (see Fig. 2). These forces are due to the airflow generated by the lateral wind. It means that the magnitude of these forces is a function of the incoming lateral airflow coming from the wind. Under the crosswind, the total thrust $f_{T_i} = f_{W_i} + f_{M_i}$, $i = 1, 2, 3, 4$, can be expressed as follows [28]:

$$f_{T_i} = 2\rho A\hat{V}V_p \tag{3}$$

where ρ is the air density and A is the propeller area, $f_{M_i} = b\Omega_i^2$ is the translational force produced by rotor i, and b is the thrust coefficient. V_p is the induced wind speed in the main propeller and $\hat{V}$ is the total induced wind speed by the rotor and lateral wind V_w, and this is given by

$$\hat{V} = \left[(V_w\cos\alpha + V_p)^2 + (V_w\sin\alpha)^2\right]^{\frac{1}{2}} \tag{4}$$

where α is the angle between the rotor axis and the lateral wind axis, and when the wind is coming from the right in the x-axis, $\alpha = 90^o$. It is important to notice that, without lateral wind, $V_w = 0$, then this gives $\hat{V} = V_p$, $f_{W_i} = 0$ and $f_{T_i} = f_{M_i}$.

Moreover, the motor torque is opposed by an aerodynamic drag, τ_{drag}. For definition, the aerodynamic drag is given by $\tau_{\text{drag}} = \rho A V_w^2/2$. Thus, the aerodynamic drag could be considered like $\tau_{\text{drag}} = k_{\text{drag}}V_w^2$, where $k_{\text{drag}} > 0$ is a constant depending on the density of air, the radius, shape of the blade and other factors. When the quadrotor is perturbed by the crosswind, the induced forces f_{W_i} in each rotor produce aerodynamical wind torques in the rotorcraft, and these moments could be expressed by $\tau_{W_\psi} = \sum_{i=1}^{4}\tau_{\text{drag}_i}$, $\tau_{W_\theta} = (f_{W_3} - f_{W_1})l$, $\tau_{W_\phi} = (f_{W_4} - f_{W_2})l$, l is the distance between the center of the quadrotor and the centre of a propeller.

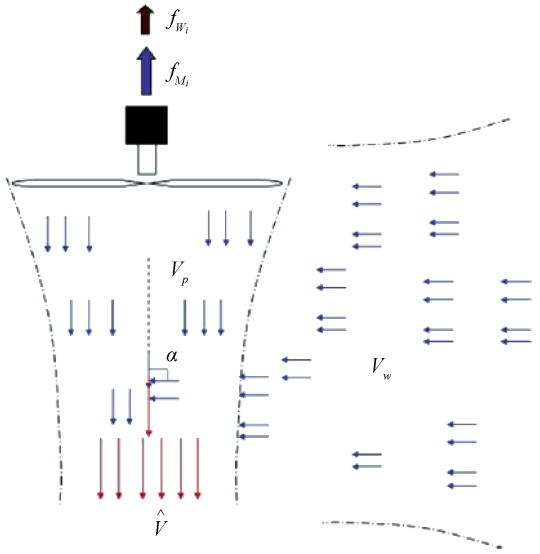

Fig. 2. Analysis of the main and lateral thrusts.

On the other hand, the gravitational force applied to the vehicle is $\boldsymbol{f}_g = -m\boldsymbol{g}\hat{\boldsymbol{k}}$, where $\hat{\boldsymbol{k}}$ denotes the unit vector codirectional with the z^E-axis, and $\boldsymbol{g}$ refers to the gravity acceleration. Therefore, one has

$$\begin{aligned}
&\boldsymbol{F} = R_{\Omega}(\sum_{i=1}^{4} f_{M_i} + \sum_{i=1}^{4} f_{W_i}) + \boldsymbol{f}_g\\
&\boldsymbol{\tau} = \boldsymbol{\tau}_A + \boldsymbol{\tau}_{W_A}
\end{aligned} \tag{5}$$

with $\boldsymbol{\tau}_A = [\tau_\psi, \tau_\theta, \tau_\phi]^T$ and $\boldsymbol{\tau}_{W_A} = [\tau_{W_\psi}, \tau_{W_\theta}, \tau_{W_\phi}]^T$.

Consequently, (1) is rewritten as follows:

$$\begin{aligned}
&m\dot{\boldsymbol{\nu}} = R_{\Omega}(\sum_{i=1}^{4} f_{M_i} + \sum_{i=1}^{4} f_{W_i}) + \boldsymbol{f}_g\\
&J\dot{\Omega} = -\Omega \times J\Omega + \Omega \times [0 \;\; 0 \;\; J_r\Omega_r] + \boldsymbol{\tau}_A + \boldsymbol{\tau}_{W_A}.
\end{aligned} \tag{6}$$

Thus, developing (5) and (6), it follows that

$$\begin{aligned}
\ddot{x} &= (\sin\psi\sin\phi + \cos\psi\sin\theta\cos\phi)\frac{U_1}{m} + W_1\\
\ddot{y} &= (-\cos\psi\sin\phi + \sin\psi\sin\theta\cos\phi)\frac{U_1}{m} + W_1\\
\ddot{z} &= -g + (\cos\theta\cos\phi)\frac{U_1}{m} + W_1\\
\ddot{\phi} &= \frac{(I_{yy} - I_{zz})}{I_{xx}}\dot{\theta}\dot{\phi} - \frac{J_r}{I_{xx}}\dot{\theta}\Omega_r + \frac{U_2}{I_{xx}} + W_2\\
\ddot{\theta} &= \frac{(I_{zz} - I_{xx})}{I_{yy}}\dot{\psi}\dot{\phi} - \frac{J_r}{I_{yy}}\dot{\phi}\Omega_r + \frac{U_3}{I_{yy}} + W_3\\
\ddot{\psi} &= \frac{(I_{xx} - I_{yy})}{I_{zz}}\dot{\phi}\dot{\theta} + \frac{U_4}{I_{zz}} + W_4
\end{aligned} \tag{7}$$

where $\boldsymbol{W} = [W_1, W_2, W_3, W_4]^T$ is the perturbed vector induced by wind, and it is defined as follows:

$$\boldsymbol{W} = \begin{bmatrix} \sum_{i=1}^{4} f_{W_i}/m \\ \dfrac{l(f_{W_4}^2 - f_{W_2}^2)}{I_{xx}} \\ \dfrac{l(f_{W_3}^2 - f_{W_1}^2)}{I_{yy}} \\ \dfrac{\sum_{i=1}^{4} \tau_{\mathrm{drag}_i}}{I_{zz}} \end{bmatrix} \tag{8}$$

where I_{xx}, I_{yy} and I_{zz} denote the inertia moments in the body-fixed frame, and the propellers' speed inputs are given through (9),

$$\begin{aligned} U_1 &= b(\Omega_1^2 + \Omega_2^2 + \Omega_3^2 + \Omega_4^2) \\ U_2 &= lb(-\Omega_2^2 + \Omega_4^2) \\ U_3 &= lb(-\Omega_1^2 + \Omega_3^2) \\ U_4 &= d(-\Omega_1^2 + \Omega_2^2 - \Omega_3^2 + \Omega_4^2) \end{aligned} \tag{9}$$

where b and d are the thrust and the drag factors, respectively. U_1 denotes the normalized total lift force, and U_2, U_3 and U_4 correspond to the control inputs of the roll, the pitch and the yaw moments, respectively. Then, rearranging the (9) in a matrix form

$$\boldsymbol{U} = L\boldsymbol{F}_M \tag{10}$$

where $\boldsymbol{U} = [U_1 \;\; U_2 \;\; U_3 \;\; U_4]^T$ is the movement vector and $\boldsymbol{F}_M = [f_{M_1} \;\; f_{M_2} \;\; f_{M_3} \;\; f_{M_4}]^T$ is the thrust vector with $f_{M_i} = b\Omega_i^2, i = 1, 2, 3, 4$. The constant matrix L is defined according to

$$L = \begin{bmatrix} 1 & 1 & 1 & 1 \\ 0 & -l & 0 & l \\ -l & 0 & l & 0 \\ -\dfrac{d}{b} & \dfrac{d}{b} & -\dfrac{d}{b} & \dfrac{d}{b} \end{bmatrix}. \tag{11}$$

C. Actuator Dynamic Model With Loss of Effectiveness (LOE) Fault

The rotors are driven by DC motors, and with the assumption that the thrust dynamics for all the actuators are identical, and from $f_{M_i} = b\Omega_i^2$, one has

$$\dot{f}_{M_i} = 2b\Omega_i\dot{\Omega}_i. \tag{12}$$

The nonlinear and linearized dynamic equations of the propeller angular speed Ω_i and the thrust $\boldsymbol{F}_M$ around an operating point $\boldsymbol{F}_0$ are provided in [19] and [29], and interested readers can refer to the two references for details. So, for the sake of brevity, the paper presents the linearized dynamic equation of the input voltage $\boldsymbol{u}$ to the thrust $\boldsymbol{F}_M$ in (13)

$$\dot{\boldsymbol{F}}_M = -A\boldsymbol{F}_M + B\boldsymbol{u} + C \tag{13}$$

where A, B and C are constant matrices and $\boldsymbol{u} = [u_1 \;\; u_2 \;\; u_3 \;\; u_4]^T$ is defined as the vector of the input voltages to the propellers.

Considering (10) and (13), the following equation is obtained

$$\begin{aligned} \dot{\boldsymbol{U}} &= -A\boldsymbol{U} + LB\boldsymbol{u} + LC \\ &= -A_0\boldsymbol{U} + B_0\boldsymbol{u} + C_0 \end{aligned} \tag{14}$$

where $A = A_0 = A_t I_{4\times4}, LB = B_0 = B_t I_{4\times4}, LC = C_0 = C_t[1 \;\; 1 \;\; 1 \;\; 1]^T$, and the parameters A_t, B_t and C_t are the linearized coefficients.

The LOE fault is characterized by a decrease in the actuator gain from its nominal value. In case of a LOE fault, the speed of the quadrotor deviates from the commanded output that is desired by the controller. In other words, one instead has

$$\Omega_i = k_{ai}\Omega_{ci}, \qquad 0 < k_{ai} < 1 \tag{15}$$

where Ω_i refers to the actual output from the ith actuator and Ω_{ci} is the commanded output by the controller and k_{ai} represents the LOE fault gain. Therefore, the resulting thrust force from this actuator changes according to the (16)

$$f_{M_i} = b\Omega_i^2 = b(k_{ai}\Omega_{ci})^2. \tag{16}$$

Then, one has

$$\dot{f}_{M_i} = 2bk_{ai}^2\Omega_{ci}\dot{\Omega}_{ci}. \tag{17}$$

Therefore the dynamics of $\boldsymbol{F}_M$ defined in (13) would also change due to the LOE fault, so (14) can be rewritten as follows:

$$\dot{\boldsymbol{U}} = -A_f\boldsymbol{U} + B_f\boldsymbol{u} + C_0 \tag{18}$$

where A_f =diag$\{A_{t1} \;\; A_{t2} \;\; A_{t3} \;\; A_{t4}\}$ and B_f =diag$\{B_{t1} \;\; B_{t2} \;\; B_{t3} \;\; B_{t4}\}$ are coefficient matrices.

Remark 1: In this paper, it is assumed that the only coefficients subject to change due to a fault are A_0, B_0, while the coefficient C_0 would remain unaffected. If the actuators have the same parameters, in other words, $A_{ti} = A_t$ and $B_{ti} = B_t$ for $i = 1, 2, 3, 4$, then the system is healthy, otherwise an actuator fault occurs.

Remark 2: It should be noted that if the actuators do not have the same characteristics, it is necessary to derive the dynamic equations of the movement vector, then the thrust dynamics for all the actuators are not identical since the dynamic equations of the movement vector $\boldsymbol{U}$ change.

III. Robust Nonlinear Recovery Controller Design

Although ADRC inherits from proportional–integral–derivative (PID) control, it has unique qualities that makes it such a success. These unique qualities are: the error-driven, rather than model-based, control law; it offers the best state observer; it embraces the power of nonlinear feedback and puts it to full use; it is a useful digital control technology developed out of an experimental platform rooted in computer simulations. The normal ADRC consists of a tracking differentiator (TD), an extended state observer (ESO) and a nonlinear state error feedback (NLSEF). However, in the real world, there are always measurement noises in control systems. Motivated by this fact, an improved ADRC control strategy is developed in this section. That is, using nonlinear function fal$(\cdot)$ given in

(24) to filter out the measurement noises. The improved ESO can not only estimate states of plant and overall disturbances, but also efficiently filter out measurement noises in systems.

Equation (7) is recalled and rewritten as follows:

$$\begin{aligned}
&\ddot{z} = f_1(z,\dot{z}) + b_1U_1 - g + W_1\\
&\ddot{\phi} = f_2(\phi,\dot{\phi},\theta,\dot{\theta},\psi,\dot{\psi}) + b_2U_2 + W_2\\
&\ddot{\theta} = f_3(\phi,\dot{\phi},\theta,\dot{\theta},\psi,\dot{\psi}) + b_3U_3 + W_3\\
&\ddot{\psi} = f_4(\phi,\dot{\phi},\theta,\dot{\theta},\psi,\dot{\psi}) + b_4U_4 + W_4
\end{aligned} \tag{19}$$

where $f_i(\cdot)$ and W_i denote the internal dynamics disturbance (such as modeling errors) and the external disturbance (i.e., wind gust), $i = 1,2,3,4$, respectively. $b_1 = \cos\theta\cos\phi/m$, $b_2 = 1/I_{xx}$, $b_3 = 1/I_{yy}$, $b_4 = 1/I_{zz}$.

The control strategy design, for example the roll control, is developed as follows. For the roll control, considering the second order system as follows:

$$\begin{aligned}
&\ddot{x} = f(x,\dot{x},\boldsymbol{W}) + b\boldsymbol{U}\\
&y = y_0 + v_y
\end{aligned} \tag{20}$$

where $f(x,\dot{x},\boldsymbol{W})$, or simply denoted as f, represents both the internal dynamics and the external disturbance, v_y denotes measurement noises, x is system state, and for the roll control, one has

$$\begin{aligned}
&\ddot{\phi} = f(\phi,\dot{\phi},\theta,\dot{\theta},\psi,\dot{\psi},\boldsymbol{W}) + b\boldsymbol{U}\\
&y = \phi_d + v_y
\end{aligned} \tag{21}$$

where ϕ_d is desired values.

A. Tracking-differentiator (TD)

In the transition design, both the transition signal v_1 and its derivative v_2 are simultaneously given. A nonlinear TD was constructed based on the fact that the numerical integration provides more stable and accurate results than numerical differentiation in the presence of noises.

Considering the roll control for the design, a second-order TD can be designed as follows:

$$\begin{aligned}
&v_1(k+1) = v_1(k) + Tv_2(k)\\
&v_2(k+1) = v_2(k) + T\mathrm{fst}(v_2(k) - v, v_2(k), r, h)
\end{aligned} \tag{22}$$

where $v = \phi_d$ is the expected output, v_1 is the tracking of v, and v_2 is the derivative of v_1. T is the sampling period, and r and h are adjusted accordingly as filter coefficients. The function $\mathrm{fst}(\cdot)$ is defined as follows:

$$\mathrm{fst}(x_1,x_2,r,h) = -\begin{cases} r\,a/d, & a \le d_0\\ r\,\mathrm{sgn}a, & a > d_0 \end{cases}$$

with

$$d = rh, d_0 = dh, \bar{y} = x_1 + hx_2, a_0 = (d^2 + 8r|\bar{y}|)^{\frac{1}{2}}$$

$$a = -\begin{cases} x_2 + \dfrac{(a_0 - d)}{2}, & |\bar{y}| > d_0\\ x_2 + \dfrac{\bar{y}}{h}, & |\bar{y}| \le d_0. \end{cases}$$

B. Improved extended-state-observer (ESO) with $\mathrm{fal}(\cdot)$ *filter*

To suppress the measurement noises, an improved ESO with $\mathrm{fal}(\cdot)$ filter is designed as follows:

$$\begin{aligned}
&y_0(k) = \mathrm{fal\,filter}(y, k_f, a_f, \delta_f)\\
&\varepsilon_1 = z_1(k) - y_0(k)\\
&z_1(k+1) = z_1(k) + T(z_2(k) - \beta_1\varepsilon_1)\\
&z_2(k+1) = z_2(k) + T(z_3(k) - \beta_2\,\mathrm{fal}(\varepsilon_1,\alpha_1,\delta) + bu(k))\\
&z_3(k+1) = z_3(k) + T\beta_3\,\mathrm{fal}(\varepsilon_1,\alpha_2,\delta)
\end{aligned} \tag{23}$$

where z_1 is the estimated state, and z_2 is the derivative of z_1, z_3 is the overall estimated uncertainties of the plant which will serve as a compensating term for the input. $\alpha_1 = 0.5$, $\alpha_2 = 0.25$. β_1, β_2, β_3 and δ are positive scalars. y_0 are filtered outputs of system. k_f, a_f and δ_f are filtering parameters, and ε_1 are errors of estimation. The nonlinear function $\mathrm{fal}(\cdot)$ [26] is given in (24).

C. Nonlinear state error feedback (NLSEF)

$$\begin{aligned}
&e_1 = v_1(k) - z_1(k)\\
&e_2 = v_2(k) - z_2(k)\\
&u_0(k) = k_1\mathrm{fal}(e_1,\alpha_1,\delta_0) + k_2\mathrm{fal}(e_2,\alpha_2,\delta_0)\\
&u(k) = u_0(k) - \frac{z_3(k)}{b}
\end{aligned} \tag{24}$$

with

$$\mathrm{fal}(\varepsilon,\alpha,\delta) = -\begin{cases} |\varepsilon|^{\alpha}\mathrm{sgn}(\varepsilon), & |\varepsilon| > \delta > 0,\\ \dfrac{\varepsilon}{\delta^{1-\alpha}}, & |\varepsilon| \le \delta > 0 \end{cases}$$

where k_1 and k_2 are positive scalars, $\alpha_1 = 0.75$ or 0.5 and $\alpha_2 = 1.25$ or 1.5. δ is positive scalar. $\mathrm{fal}(\cdot)$ is a nonlinear function, and when $\alpha < 1$, it has the advantages of small error, large gain and large error, small gain.

IV. Simulation Results

In order to validate the fault recovery and disturbance rejection capabilities of the proposed control strategy for stabilizing the quadrotor at hovering, the following two simulation conditions are considered with the parameters of the quadrotor referred from [30].

1) Lateral wind gusts are applied with wind velocity $V_W = 9\,m/s$ at a specific time window $\Delta T = [5,7]$ seconds. The sampling period is set to $T = 0.01\,s$. The initial values are: $\phi_0 = 15^\circ$, $\theta_0 = 10^\circ$, $\psi_0 = 30^\circ$. The white Gaussian noise with zero mean value and variance of 0.01 is applied to describe measurement noises. While at hovering, the desired values are: $z_d = 1\,m$, $\phi_d = 0^\circ$, $\theta_d = 0^\circ$ and $\psi_d = 0^\circ$. The simulation results are shown in Figs. 3−10. From Fig. 3, one can see that ADRC-based control has no overshoot as compared to nonlinear PID-based control with filter. Figs. 5, 7 and 9 show that ADRC-based control can compensate the perturbations resulted from wind gusts through the estimations provided by ESO, therefore, ADRC-based control can effectively stabilize and achieve accurate attitude control even though there are forceful wind gusts at time window $\Delta T = [5,7]$ seconds. Figs. 4, 6 and 8 illustrate that improved ESO can efficiently estimate system states and the amplitude of the wind disturbances.

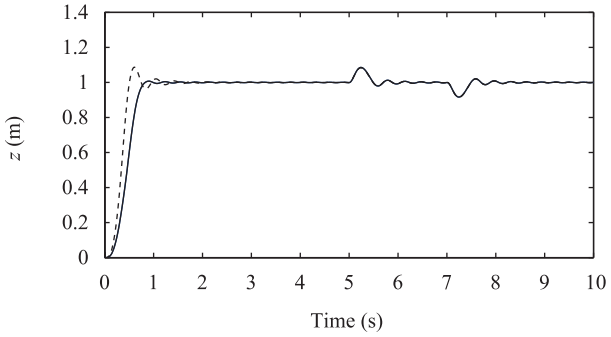

Fig. 3. Outputs of vertical position z: ADRC-based control (solid line); nonlinear PID-based control (dashed line).

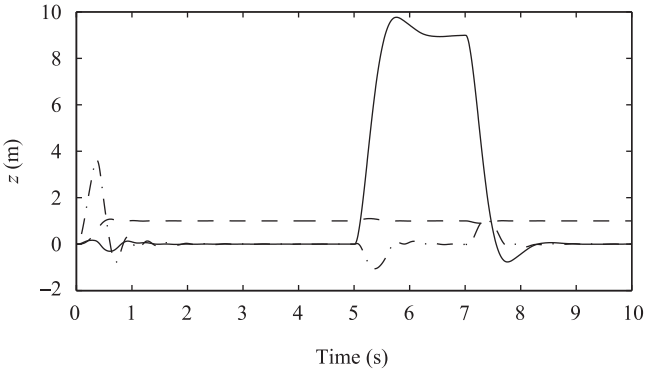

Fig. 4. Outputs of ESO for z: z_1-the estimated states of system (dotted line); z_2-the differential of z_1 (dash-dot line); z_3-the estimated overall disturbances (solid line).

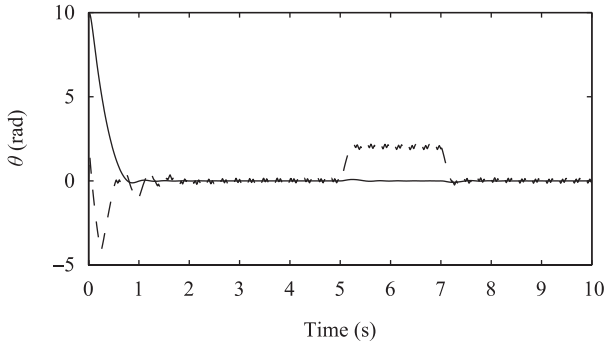

Fig. 5. Outputs of pitch angle θ: ADRC-based control (solid line); nonlinear PID-based control (dashed line).

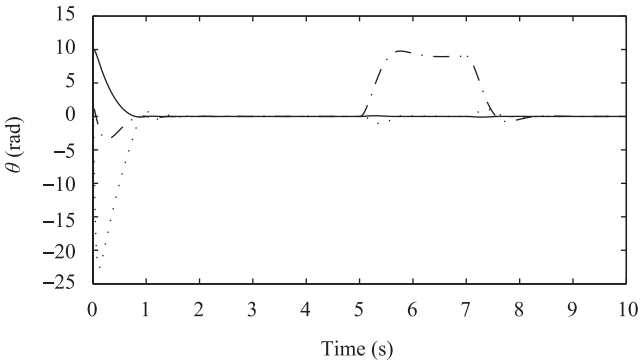

Fig. 6. Outputs of ESO for θ: z_1-the estimated states of system (solid line); z_2-the differential of z_1 (dashed line); z_3-the estimated overall disturbances (dash-dot line).

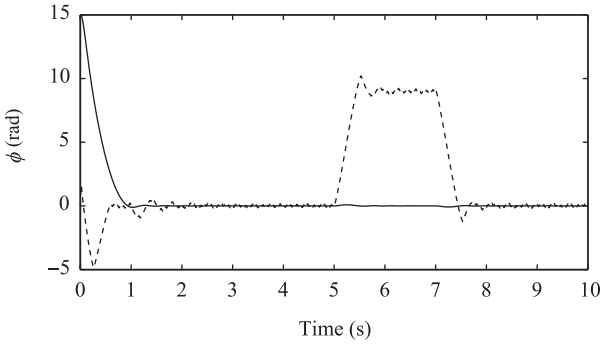

Fig. 7. Outputs of roll angle ϕ: ADRC-based control (solid line); nonlinear PID-based control (dashed line).

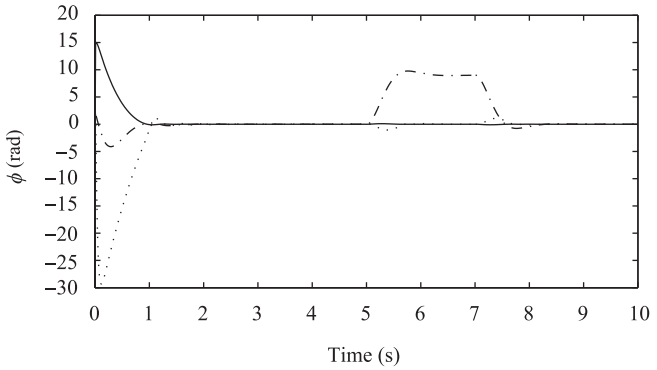

Fig. 8. Outputs of ESO for ϕ: z_1-the estimated states of system (solid line); z_2-the differential of z_1 (dashed line); z_3-the estimated overall disturbances (dash-dot line).

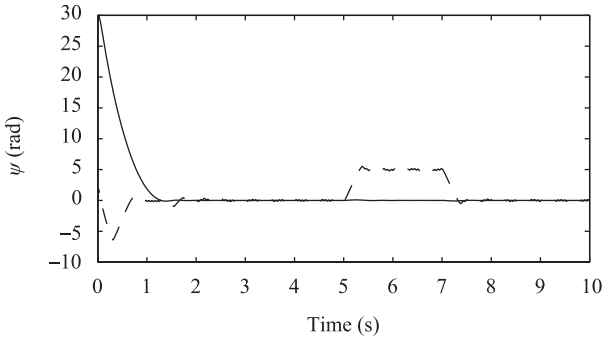

Fig. 9. Outputs of yaw angle ψ: ADRC-based control (solid line); nonlinear PID-based control (dashed line).

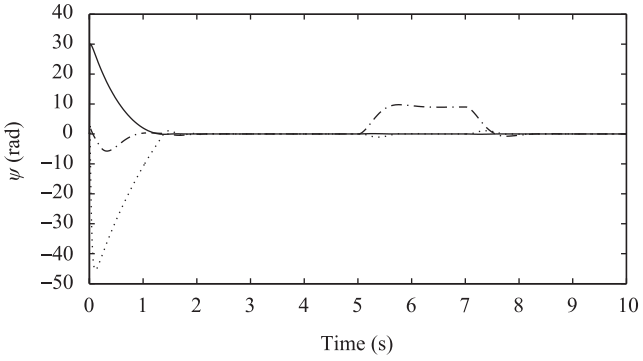

Fig. 10. Outputs of ESO for ψ: z_1-the estimated states of system (solid line); z_2-the differential of z_1 (dashed line); z_3-the estimated overall disturbances (dash-dot line).

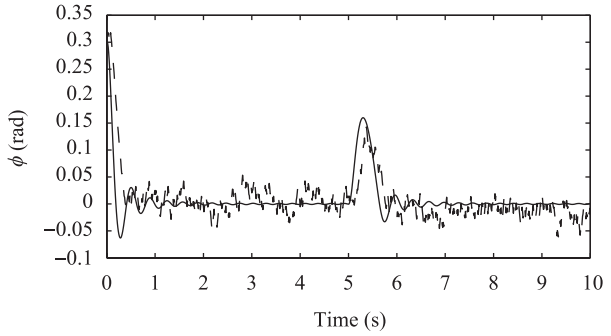

Fig. 11. Outputs of roll angle ϕ after fault recovery: ADRC based fault tolerant control (solid line); nonlinear PID based fault tolerant control (dashed line).

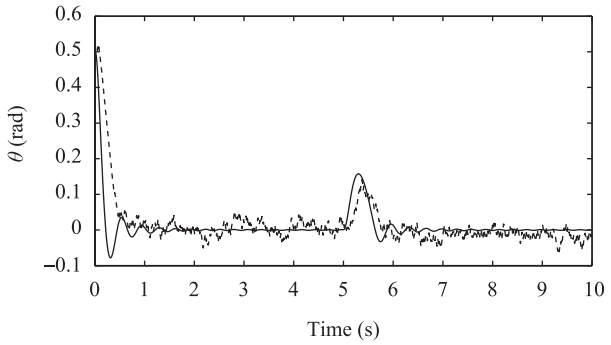

Fig. 12. Outputs of pitch angle θ after fault recovery: ADRC based fault tolerant control (solid line); nonlinear PID based fault tolerant control (dashed line).

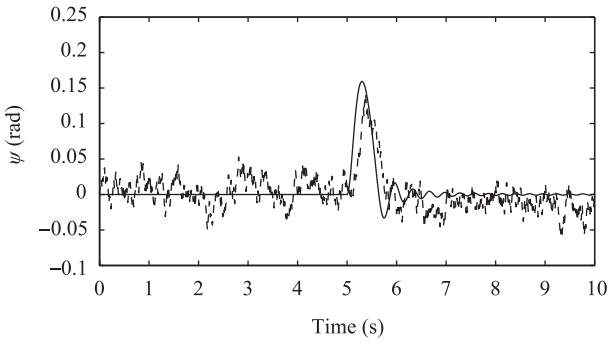

Fig. 13. Outputs of yaw angle ψ (rad) after fault recovery: ADRC based fault tolerant control (solid line); nonlinear PID based fault tolerant control (dashed line).

2) The fault considered here assumes a 25 % LOE in the first actuator at $t = 5\,\text{sec}$. While at hovering, the desired values are: $z_d = 3\,m$, $\phi_d = 0^\circ$, $\theta_d = 0^\circ$ and $\psi_d = 0^\circ$. The white Gaussian noise with zero mean value and variance of 0.01 is applied to describe measurement noises. Figs. 11−15 show the outputs of quadrotor helicopter with measurement noises and actuator fault. From these figures, one can see that when actuator fault occurs, ADRC-based fault tolerant controller can still accurately control the attitude angles, since it can remarkably deal with the completely unknown uncertainties

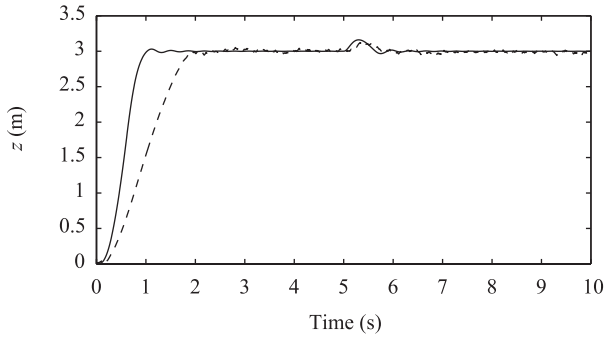

Fig. 14. Outputs of vertical position z after fault recovery: ADRC based fault tolerant control (solid line); nonlinear PID based fault tolerant control (dashed line).

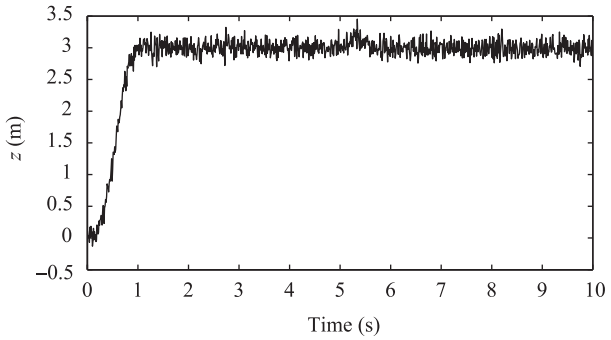

Fig. 15. Outputs of vertical position z after fault recovery with ADRC fault tolerant control but without filtering.

that come from both the internal and external, and it regards actuator fault as unknown uncertainties, then through compensating the uncertainties induced by the actuator faults to recover the performance of faulty system. However, comparing with ADRC-based fault tolerant control, nonlinear PID-based fault tolerant control (without filter) has larger delay, and meanwhile, it is affected seriously by measurement noises. Moreover, the attitudes are not stabilized well by nonlinear PID-based fault tolerant controller. From Figs. 14 (solid line) and 15, it is clear that measurement noises are well rejected by improved ESO with nonlinear function filter.

V. Conclusion

In this paper, a novel robust fault tolerant control strategy based on ADRC is successfully applied to stabilize an unmanned quadrotor aircraft subjecting to actuator faults and wind gusts. An improved ESO is designed to estimate the plant dynamics and disturbances, while a nonlinear feedback control law is developed to actively suppress disturbances and accommodate actuator faults. With the accurate estimation of the plant dynamics and disturbances by ESO, the developed controller can successfully drive the outputs of quadrotor aircraft to the desired values. The proposed algorithms are validated through simulation, and the results obtained from simulation demonstrated the effectiveness of the developed control algorithm dealing with the completely unknown uncertainties that come from both internal faults and external disturbances. However, there are so many parameters of ADRC which should be carefully tuned, so ADRC with parameter adaption

will be one of the focuses of our future work, also, experiments need to be carried out for fault recovery in presence of real wind (outdoor).

REFERENCES

[1] D. W. Murphy and J. Cycon, "Applications for mini VTOL UAV for law enforcement," in *Proc. SPIE 3577, Sensors, C3I, Information, and Training Technologies for Law Enforcement*, Boston, MA, USA, 1999.

[2] Committee on Autonomous Vehicles in Support of Naval Operations, National Research Council, *Autonomous Vehicles in Support of Naval Operations*. Washington DC: The National Academies Press, 2005.

[3] G. Slater, "Cooperation between UAVs in a search and destroy mission," in *AIAA Guidance, Navigation, and Control Conf. and Exhibit*, Austin, Texas, USA, 2003.

[4] S. R. Herwitz, L. F. Johnson, S. E. Dunagan, R. G. Higgins, D. V. Sullivan, J. Zheng, B. M. Lobitz, J. G. Leung, B. A. Gallmeyer, M. Aoyagi, R. E. Slye, and J. A. Brass, "Imaging from an unmanned aerial vehicle: Agricultural surveillance and decision support," *Comput. Electron. Agric.*, vol. 44, no. 1, pp. 49−61, Jul. 2004.

[5] J. H. Kim and S. Sukkarieh, "Airborne simultaneous localisation and map building," in *Proc. IEEE Int. Conf. Robotics and Automation*, Taipei, Taiwan, China, 2003, vol. 1, pp. 406−411.

[6] K. Alexis, G. Nikolakopoulos, A. Tzes, and L. Dritsas, "Coordination of helicopter UAVs for aerial forest-fire surveillance," in *Applications of Intelligent Control to Engineering Systems*, K. P. Valavanis, Ed. Netherlands: Springer, 2009, pp. 169−193.

[7] C. Yuan, Y. M. Zhang, and Z. X. Liu, "A survey on technologies for automatic forest fire monitoring, detection, and fighting using unmanned aerial vehicles and remote sensing techniques," *Can. J. For. Res.*, vol. 45, no. 7, pp. 783−792, Mar. 2015.

[8] N. Metni and T. Hamel, "A UAV for bridge inspection: Visual servoing control law with orientation limits," *Automat. Construct.*, vol. 17, no. 1, pp. 3−10, Nov. 2007.

[9] Z. Sarris, "Survey of UAV applications in civil markets," in *Proc. the 9th Mediterranean Conf. Control and Automation*, Dubrovnik, Croatia, 2001.

[10] X. Wang and Y. M. Zhang, "A survey on remote sensing and computer vision technologies for automatic power line inspection using unmanned aerial vehicles," in *Proc. the 12th Int. Conf. Intelligent Unmanned System*, Xi'an, China, 2016.

[11] J. R. Azinheira and A. Moutinho, "Hover control of an UAV with backstepping design including input saturations," *IEEE Trans. Control Syst. Technol.*, vol. 16, no. 3, pp. 517−526, Apr. 2008.

[12] S. Jackson, J. Tisdale, M. Kamgarpour, B. Basso, and J. K. Hedrick, "Tracking controllers for small UAVs with wind disturbances: Theory and flight results," in *Proc. the 47th IEEE Conf. Decision and Control*, Cancun, Mexico, 2008, pp. 564−569.

[13] A. L. Jennings, R. Ordonez, and N. Ceccarelli, "An ant colony optimization using training data applied to UAV way point path planning in wind," in *Proc. IEEE Swarm Intelligence Symp.*, St. Louis, MO, USA, 2008, pp. 1−8.

[14] M. D. Hua, T. Hamel, P. Morin, and C. Samson, "A control approach for thrust-propelled underactuated vehicles and its application to VTOL drones," *IEEE Trans. Automat. Control*, vol. 54, no. 8, pp. 1837−1853, Aug. 2009.

[15] K. Alexis, G. Nikolakopoulos, and A. Tzes, "Experimental model predictive attitude tracking control of a quadrotor helicopter subject to wind-gusts," in *Proc. the 18th Mediterranean Conf. Control & Automation*, Marrakech, Morocco, 2010, pp. 1461−1466.

[16] K. Alexis, G. Nikolakopoulos, and A. Tzes, "Constrained-control of a quadrotor helicopter for trajectory tracking under wind-gust disturbances," in *Prco. 2010 the 15th IEEE Mediterranean Electrotechnical Conf. MELECON*, Valletta, Malta, 2010, 1411−1416.

[17] D. H. Zhou, Y. Liu, and X. He, "Review on fault diagnosis techniques for closed-loop systems," *Acta Automat. Sin.*, vol. 39, no. 11, pp. 1933−1943, Nov. 2013.

[18] Y. Y. Guo and B. Jiang, "Multiple model-based adaptive reconfiguration control for actuator fault," *Acta Automat. Sin.*, vol. 35, no. 11, pp. 1452−1458, Nov. 2009.

[19] M. Ranjbaran and K. Khorasani, "Generalized fault recovery of an under-actuated quadrotor aerial vehicle," in *Proc. 2012 American Control Conf.*, Montreal, Canada, 2012, 2515−2520.

[20] M. Y. Zhong, S. X. Ding, and D. H. Zhou, "A new scheme of fault detection for linear discrete time-varying systems," *IEEE Trans. Automat. Control*, vol. 61, no. 9, pp. 2597−2602, Sep. 2014.

[21] Y. Y. Guo, Y. M. Zhang, and B. Jiang, "Set-membership estimation-based adaptive reconfiguration scheme for linear systems with disturbances," *Int. J. Adapt. Control Signal Process.*, vol. 30, no. 2, pp. 359−374, Aug. 2016.

[22] M. H. Amoozgar, A. Chamseddine, and Y. M. Zhang, "Fault-tolerant fuzzy gain-scheduled PID for a quadrotor helicopter testbed in the presence of actuator faults," *IFAC Proc. Volumes*, vol. 45, no. 3, pp. 282−287, 2012.

[23] J. M. Maciejowski and C. N. Jones, "MPC fault-tolerant flight control case study: flight 1862," in *Proc. the 5th Symp. Fault Detection, Supervision and Safety for Technical Processes*, Washington D.C., USA, 2003.

[24] T. Li, Y. M. Zhang, and B. Gordon, "Fault tolerant control applied to a quadrotor unmanned helicopter," in *Proc. ASME/IEEE International Conference on Mechatronic and Embedded Systems and Applications*, Washington D.C., USA, 2011.

[25] H. Bouadi, M. Bouchoucha, and M. Tadjine, "Sliding mode control based on backstepping approach for an UAV type quadrotor," *Int. J. Appl. Math. Comput. Sci.*, vol. 4, no. 1, pp. 12−17, 2007.

[26] J. Q. Han, "From PID technique to active disturbances rejection control technique," *Control Eng. China*, vol. 9, no. 3, pp. 13−18, May 2002.

[27] L. E. Muñoz, P. Castillo, G. Sanahuja, and O. Santos, "Embedded robust nonlinear control for a four-rotor rotorcraft: validation in real-time with wind disturbances," in *Proc. 2011 IEEE/RSJ Int. Conf. Intelligent Robots and Systems*, San Francisco, CA, USA, 2011, 2682−2687.

[28] S. Salazar, H. Romero, R. Lozano, and P. Castillo, "Modeling and real-time stabilization of an aircraft having eight rotors," *J. Intell. Robot. Syst.*, vol. 54, no. 1−3, pp. 455−470, Mar. 2009.

[29] T. Bresciani, "Modelling, identification and control of a quadrotor helicopter," M.S. thesis, Dept. Automat. Control, Lund Univ., Lund, 2008, 22−27.

[30] Y. L. He, Y. M. Chen, and M. F. Zhou, "Modeling and control of a quadrotor helicopter under impact of wind disturbance," *J. Chin. Inert. Technol.*, vol. 21, no. 5, pp. 624−630, Oct. 2013.

Yuying Guo received the M.S. and Ph.D. degrees from Jilin University, and Nanjing University of Aeronautics and Astronautics, in 2003, and 2010, respectively. From 2013 to 2014, supported by the China Scholarship Council, she was a postdoctoral research fellow with Concordia University, Montreal, QC, Canada. She joined the School of Information Engineering as an Associate Professor, Southwest University of Science and Technology, in September 2003. Her current research interests include nonlinear control, fault diagnosis, fault-tolerant control systems, and their applications to fight control.

Bin Jiang (M'00-SM'06) was born in Jiangxi, China, in 1966. He obtained the Ph.D. degree in automatic control from Northeastern University, Shenyang, China, in 1995. He had been Postdoctoral Fellow, Research Fellow, Invited Professor and Visiting Professor in Singapore, France, USA and Canada, respectively. Now he is a Chair Professor of Cheung Kong Scholar Program in Ministry of Education and Dean of the College of Automation Engineering in Nanjing University of Aeronautics and Astronautics, China. He currently serves as Associate Editor or Editorial Board Member for a number of journals such as *IEEE Trans. on Control Systems Technology*; *IEEE Trans. on Fuzzy Systems*; *Int. J. of Control*, *Automation and Systems*; *Nonlinear Analysis*: *Hybrid Systems*; *Int. J. of Applied Mathematics and Computer Science*; *Mathematical Problem in Engineering*; *Acta Automatica Sinica*; *Journal of Astronautics*. He is the Chair of Control Systems Chapter in IEEE Nanjing Section, a member of IFAC Technical Committee on Fault Detection, Supervision, and Safety of Technical Processes. His research interests include intelligent fault diagnosis and fault tolerant control and their applications.

Youmin Zhang (M'99-SM'07) received the B.S., M.S., and Ph.D. degrees from Northwestern Polytechnical University, Xi'an, China, in 1983, 1986, and 1995, respectively. He is currently a Professor with the Department of Mechanical and Industrial Engineering and the Concordia Institute of Aerospace Design and Innovation, Faculty of Engineering and Computer Science, Concordia University, Montreal, Quebec, Canada. His current research interests include condition monitoring, health management, fault diagnosis, and fault-tolerant (flight) control systems, cooperative guidance, navigation, and control (GNC) and remote sensing of single and multiple unmanned aerial/space/ground/surface vehicles and their applications to forest fires, powerlines and pipelines, search and rescue monitoring, detection and services, dynamic systems modeling, estimation, identification, advanced control techniques and advanced signal processing techniques for diagnosis, prognosis, and health management of safety-critical systems, renewable energy systems and smart grids, and manufacturing processes. He has authored four books, over 460 journal and conference papers, and book chapters. He is a Fellow of Canadian Society of Mechanical Engineering (CSME), a Senior Member of the American Institute of Aeronautics and Astronautics (AIAA) and the Institute of Electrical and Electronics Engineers (IEEE), and a member of the Technical Committee (TC) for several scientific societies, including the International Federation of Automatic Control TC on Fault Detection, Supervision and Safety for Technical Processes, the AIAA Infotech@Aerospace Program Committee on Unmanned Systems, the IEEE Robotics and Automation Society TC on Aerial Robotics and Unmanned Aerial Vehicles, the ASME/IEEE TC on Mechatronics and Embedded Systems and Applications, and the International Conference on Unmanned Aircraft Systems (ICUAS) Association Executive Committee. He has been invited to deliver plenary talks at international conferences/workshops and research seminars worldwide for over 90 times. He is an Editor-in-Chief of the *Journal of Instrumentation*, *Automation and Systems*, an Editor-at-Large of the *Journal of Intelligent and Robotic Systems*, and an Editorial Board Member/Associate Editor of several other international journals (including three newly launched journals on Unmanned Systems). He has served as General Chair, Program Chair, and IPC Member of many international conferences, including the General Chair of the 10th International Conference on Intelligent Unmanned Systems (ICIUS) in 2014, Montreal, Canada, the Program Chair of the International Conference on Unmanned Aircraft Systems (ICUAS) in 2014, Orlando, FL, USA, one of General Chairs of the ICUAS in 2015, Denver, USA, a Co-General Chair of the ICIUS 2016 held at Xian, China, a Program Co-Chair for the SDPC 2017, Shanghai, China, Program Chair of the ICUAS 2017 held at Miami, USA, and General Chair of the ICUAS 2018 to be held at Dallas, USA during June 12−15, 2018. More detailed information can be found at http://users.encs.concordia.ca/ ymzhang/.